J. Biochem. 2010;147(5):661–669 doi:10.1093/jb/mvp209

JB THE JOURNAL OF BIOCHEMISTRY

Characterization of site-specific mutants of alkylhydroperoxide reductase with dual functionality from *Helicobacter pylori*

Received December 3, 2009; accepted December 16, 2009; published online January 4, 2010

Chun-Hao Huang[1], Ming-Hong Chuang[2], Yuan-Heng Wu[2], Wei-Chu Chuang[3], Pei-Jhen Jhuang[3] and Shyh-Horng Chiou[1,2,3,*]

[1]Institute of Biological Chemistry, Academia Sinica, Taipei 115, [2]Institute of Biochemical Sciences, National Taiwan University, Taipei 106 and [3]Graduate Institute of Medicine and Center for Research Resources and Development, Kaohsiung Medical University, Kaohsiung 807, Taiwan

*S.-H. Chiou, Center for Research Resources and Development, Kaohsiung Medical University, Kaohsiung 807 or Institute of Biological Chemistry, Academia Sinica, Taipei 115, Taiwan. Tel: +886-7-3133874, Fax: +886-7-3133434, email: shchiou@kmu.edu.tw

Alkylhydroperoxide reductase (AhpC) is an abundant and important antioxidant protein present in *Helicobacter pylori* (HP), a spiral Gram-negative microaerophilic bacterium. By sequence alignment and structure comparison, HP-AhpC was found to be more homologous to human peroxiredoxins (hPrx) than to other eubacterial AhpC proteins. Similar to hPrxI, native HP-AhpC existed as a dimer of single subunit, comprising α-helix and β-sheet domains with low surface hydrophobicity. AhpC can form high-molecular-weight (HMW) aggregates ranging from 700 to higher than 2,000 kDa under oxidative stress, possessing chaperone activity in the presence of thioredoxin (Trx). Further analysis of peroxide-reductase activities showed that HP-AhpC was more resistant to H_2O_2 than hPrxI. However, the mechanism of enzyme inactivation to H_2O_2 appeared to be similar for both HP-AhpC and hPrxI as revealed by native gel electrophoresis followed by proteomic identification using two-dimensional gel electrophoresis (2-DE) and LC-MS/MS. In contrast to T90D-hPrxI mutant with chaperone activity, site-specific mutant T87D-HP-AhpC did not form HMW chaperone complexes. The comparison of these two evolutionarily distant and yet functionally related enzymes may shed some light on the mechanism(s) underlying the evolution and development of the dual functionality in HP-AhpC and hPrxI with similar protein structure.

Keywords: alkylhydroperoxide reductase/chaperone/*Helicobacter pylori*/oxidative stress/peroxiredoxin.

Abbreviations: AhpC, alkylhydroperoxide reductase; 2-DE, two-dimensional polyacrylamide gel electrophoresis; *H. pylori*, *Helicobacter pylori*; LC-MS/MS, liquid chromatography coupled tandem mass spectrometry; Prx, peroxiredoxin; Trx, thioredoxin; TrxR, thioredoxin reductase.

Alkylhydroperoxide reductase (HP-AhpC), an important member of 2-Cys peroxiredoxin (Prx) family (*1*), is abundantly expressed in *Helicobacter pylori* for balancing the intracellular levels of reactive oxygen species (ROS) generated from metabolisms or mild environmental stresses (*2–4*). When undertaking peroxide-scavenging removal intracellularly, HP-AhpC usually makes use of thioredoxin (Trx)-dependent peroxidase activity to decompose H_2O_2 and organic peroxides (*5*,*6*). Although this reductase is ubiquitous in many bacteria (*7*,*8*), HP-AhpC is significantly different from that isolated from other prokaryotes.

Our previous study indicated that the sequence of AhpC from *H. pylori* is more homologous to mammalian Prxs than to other eubacterial AhpC (*9*). Additionally, we found that HP-AhpC also displays dual-activities, which switches from a peroxide reductase of low-molecular-weight (LMW) oligomers under microaerobic and short-term (<8 h) oxidative-shock conditions to a molecular chaperone of high-molecular-weight (HMW) complexes in the presence of Trx after long-term (>16 h) oxidative-stress stimulation. Similar phenomena have also been demonstrated in the Prxs of yeast and human (*10*, *11*).

In previous reports, hPrxI was found to be inactivated by H_2O_2 due in fact to the conversion of the active-site cysteine to Cys-SO_2H and Cys-SO_3H (*12*, *13*). Phosphorylation of Thr^{90} of hPrxI by Cdc2 (a cyclin-dependent kinase) *in vitro* exhibited higher chaperone activity at the expense of peroxidase activity (*14*). On the contrary, the corresponding Thr residue in native HP-AhpC (Thr^{87}) was found to be non-phosphorylated *in vivo* (*9* and unpublished result). These results pointed to the fact that both AhpC and hPrxI can polymerize or aggregate into HMW chaperone complexes under oxidative stress *in vivo* or *in vitro* (*15*). Although the mechanism of functional switch in eukaryote hPrxI appears to be novel and intriguing, the dual functionality associated with prokaryote HP-AhpC and hPrxI remains to be substantiated and clarified.

In the present study, we further examine the physico-chemical properties of HP-AhpC, including the estimation of molecular size of HMW aggregates and the mechanism of functional switch to a HMW chaperone. To investigate the functionality of HP-AhpC and hPrxI, we used site-directed mutagenesis to substitute AhpC-Thr^{87} with aspartate residue in order to mimic the phosphorylation status of the protein. Cysteines 49 and 169 in the active site of HP-AhpC were also singly replaced by serine residues to generate the C49S and C169S mutant enzymes. The comparative mechanistic study of two functionally

related enzymes reported herein may provide some insight into the mechanism(s) underlying the evolution and development of dual functionality in HP-AhpC and hPrxI with similar protein structure.

Materials and Methods

Materials

The *Escherichia coli* strain used for expression was Ecos21 (BL21). Protein concentrations were determined with the bicinchoninic acid (BCA) protein assay kit (Pierce, Rockford, IL, USA). Protein standards used in the polyacrylamide gel electrophoresis (1D or 2D PAGE) and gel-filtration/high performance liquid chromatography (GF-HPLC) were purchased from Amersham Pharmacia (Uppsala, Sweden). The recombinant hPrxI proteins, rabbit polyclonal anti-hPrxI antibody, 4,4′-dianilino-1,1′-binaphthyl-5,5′-disulfonate (*bis*-ANS), bacterial thioredoxin (Trx) system used in AhpC activity assays including thioredoxin, thioredoxin reductase and NADPH and H_2O_2 were obtained from Sigma (St Louis, MO, USA). The HPLC column G4000 SWXL (7.8×300 mm) was from Tosoh (Tokyo, Japan).

Sequence alignment and structure modelling

Analysis of protein sequence data and their alignment was carried out in MegAlign program module in Lasergene package (DNASTAR Inc., Madison, WI). Structure modelling was carried out using the Swiss-Model Automated Comparative Protein Modeling Server (*16*). Suitable templates were identified using the Template Identification tool with Gapped BLAST (*17*). The PDB ID of templates for HP-AhpC, hPrxI and MT-AhpC were 1ZOF (*18*), 1QMV (*19*) and 2BMX (*20*).

Bacterial strain and culture condition

The *H. pylori* strain HD30 used in this study was isolated from the gastric biopsy specimens of a patient with duodenal ulcer. *Helicobacter pylori* strain was grown on Centers for Disease Control and Prevention (CDC) anaerobic blood agar plates (BD) at 37°C in a modular atmosphere-controlled system (5% O_2/10% CO_2/85% N_2) and confirmed to be *H. pylori* because of their urease activity and helical morphology as determined by phase-contrast microscopy.

Cloning and mutation of the H. pylori ahpC gene

The *ahpC* gene was cloned from *H. pylori* genomic DNA, which was prepared from confluent *H. pylori* cultures with an UltraClean Microbial DNA isolation kit (MOBIO Labs Inc., Solana Beach, CA, USA). Single point-mutated HP-AhpC (C49S-, C169S-, T87D-HP-AhpC) DNA were generated by polymerase chain reaction-mediated mutagenesis. Primers used for site-specific mutants of HP-AhpC are shown in Table I.

Expression and purification of recombinant AhpC

For expression of HP-AhpC in *E. coli*, the yAhpC plasmid (*ahpC* of HD30 inserted into yT&A cloning vector) was doubly digested with the restriction endonucleases *Xho*I and *Nde*I, and ligated into pET21b (Novagen, Darmstadt, Germany), a His-taq protein expression vector bearing the T7 promoter and ampicillin resistance. The plasmids with the correct gene sequences were then transformed into *E. coli* strain BL21 (DE-3). The $(His)_6$-fused AhpC was expressed and then purified by using native Ni–NTA column. The purity of the purified recombinant AhpC was determined to be >99% based on SDS–PAGE and its MW determination analysed by a Beckman–Coulter XL-A analytical ultracentrifuge (AUC) with an An60Ti rotor as previously described (*21*).

Gel-filtration/high performance liquid chromatography (GF-HPLC)

Gel filtration on HPLC (Hitachi, Japan) was performed with a G4000SWXL column equilibrated with a flow rate of 0.5 ml/min at ambient temperature in 50 mM HEPES buffer (pH 7.0) containing 100 mM NaCl as described previously (*21*). Protein peaks as detected by A_{280} absorbance were isolated and concentrated using an Amicon Ultra-15 membrane. The protein size was determined in GF-HPLC by using the gel-filtration calibration kit from Amersham (Uppsala, Sweden).

Detection of structural changes in polymerization of AhpC under oxidative stress by circular dichroism (CD) and fluorescence spectroscopy

CD spectra were obtained on a Jasco J-810 spectropolarimeter (Jasco International Co., Tokyo, Japan). The temperature for CD measurement was controlled and maintained by a thermostatic, circulating water bath. Native purified and Trx-dependent oxidized AhpC of *H. pylori* dissolved in 10 mM sodium phosphate buffer (pH 7.5) to a final concentration of ~0.3 mg/ml were used for the Far- UV CD spectral analysis from 260 to 190 nm with a 0.02 cm-pathlength water-jacket cell under constant N_2 flush and constant-temperature water flow. All the spectra were recorded as the mean of five accumulations. The CD data were expressed as molar ellipticity in [θ] (deg cm^2 dmol^{-1}). The ellipticity is reported as mean residue molar ellipticity and calculated as follows:

$$[\theta] = \frac{[\theta]_{obs}(mrw)}{10cl}$$

where $[\theta]_{obs}$ is the ellipticity measured in degrees, mrw is the mean residue weight of the protein, c is the concentration (in g/ml), and l is the optical pathlength of the cell (in cm).

For the fluorescence study, we measured the exposure of hydrophobic domains of AhpC under normal and stressed conditions by the binding of *bis*-ANS (5 mM final concentration) to proteins (10 μM final concentration) in a total volume of 200 μl PBS buffer with a Jasco FP-6300 spectrofluorometer (Jasco International Co., Tokyo, Japan) fitted with a thermostatted cell cuvette. The extrinsic fluorescence spectra of *bis*-ANS binding to AhpC were measured with excitation fixed at 370 nm and emission scanned at 400–600 nm and a light slit of 2.5 nm bandwidth for both excitation and emission modes.

Peroxide reductase activity assays

The peroxide reductase activity of recombinant AhpC (rAhpC) was monitored with an Ultrospec 4000 spectrophotometer (Amersham Biosciences, Uppsala, Sweden) at 25°C by following the decrease in A_{340} within 10 min due to NADPH oxidation. Each assay was performed by using 20 μM each AhpC and its mutants plus hPrxI in a total volume of 1.0 ml of 50 mM potassium phosphate buffer (pH 7.0)/0.1 M ammonium sulfate/0.5 mM EDTA containing Trx system (5 μM thioredoxin, 0.5 μM thioredoxin reductase and 150 μM NADPH) and 1 mM H_2O_2 as described (*9*).

Gel electrophoresis and western blot analysis

For native PAGE, 0.2 μg of HP-AhpC or hPrxI proteins was dissolved in a native buffer without SDS and then applied to

Table I. List of primers used for site-specific mutants of HP-AhpC.

Genes	Forward primer	Reverse primer
Wild-type ahpC	5′-CCATATGTTAGTTACAAAACTTGCC-3′	5′-CTCGAGAAGCTTAATGGAATTTTC-3′
C49S-ahpC[a]	5′-GATTTTACTTTTGTATCCCCTACAGAAATCATTG-3′	5′-CAATGATTTCTGTAGGGGATACAAAAGTAAAATC-3′
C169S-ahpC[a]	5′-GGTGAAGTGTCTCCAGCAGGC-3′	5′-GCCTGCTGGAGACACTTCACC-3′
T87D-ahpC[a]	5′-GCATGGAAAAACGACCCTGTGGAAAAAG-3′	5′-CTTTTTCCACAGGGTCGTTTTTCCATGC-3′

Annealing temperature is 55°C for primers.
[a]Primers designed for site-specific mutants need to combine with primers of wild-type *ahpC* for mutant construction.

native gel electrophoresis. After electrophoresis, the proteins were transferred to poly-(vinylidene difluoride) (PVDF) membranes. After transfer, the membranes were saturated with 5% BSA in TBS/0.1% Tween-20 at room temperature overnight, followed by incubation with rabbit polyclonal antibodies against HP-AhpC for 1 h (*9*). After three washes with TBS/0.1% Tween-20, the membranes were incubated with a solution of anti-rabbit secondary antibody conjugated with peroxidase. After 1 h incubation at room temperature, the membranes were washed three times with TBS/0.1% Tween-20 and the membrane blots were developed by using ECL substrates (Pierce, IL).

Two-dimensional polyacrylamide gel electrophoresis (2-DE) and image analysis

Cell pellets of *H. pylori* grown under normal or stressed conditions (10 mM H_2O_2) for 3 h were solubilized in lysis buffer containing 8 M urea, 0.5% CHAPS or Triton X-100. After estimation of protein content by using a 2-D Quant Kit (Amersham Biosciences, Uppsala, Sweden), 250 µg total protein was loaded onto IPG gel strips (pH 3–10, 13 cm, Amersham Biosciences, Uppsala, Sweden). The IPG strips were rehydrated overnight according to the operation guideline of the manufacturer (Amersham Biosciences, Uppsala, Sweden). For the 1-D separation, IEF was carried out using Ettan IPGphor II (Amersham Biosciences, Uppsala, Sweden) at 20°C with 50–3500 V for 19 h. After IEF, the IPG strips were equilibrated for 10 min each in two equilibration solutions [50 mM Tris–HCl, pH 8.8, 6 M urea, 2% SDS, 30% glycerol containing 100 mg dithiothreitol (DTT) or 250 mg iodoacetic acid (IAA), respectively], attached to a 14% SDS–polyacrylamide gel of Laemmli's buffer system, then covered by 0.5% agarose gel. 2-DE was conducted at 130–250 V for 5–6 h until the bromophenol blue reached the bottom of the gel. The gels were stained by Sypro-Ruby overnight. The protein profiles of the gels were scanned using a Typhoon 9400 scanner (Amersham Biosciences, Uppsala, Sweden). Gel image matching was done using PDQuest software (Bio-Rad, Richmond, CA). Intensity levels were normalized between-gels as a proportion of the total protein intensity detected for the entire gel. The protocol of in-gel digestion and LC-MS/MS was as described in our previous report (*22*).

Results

Sequence alignment and structure comparison

We aligned seven protein sequences encompassing representative AhpC proteins and peroxiredoxins of *H. pylori* and other prokaryotic and eukaryotic organisms (Fig. 1A). The regions related to peroxidase and chaperone activities of human peroxiredoxins were designated by three stars (enclosed by squares). It is noted that HP-AhpC is more homologous to mammalian peroxiredoxins than other bacterial AhpC proteins, especially at the sequence region enclosing active sites and Thr^{87} (Thr^{90} in hPrxI). Using protein structure modeling (Fig. 1B), we have also found that the HP-AhpC is more similar structurally to mammalian peroxiredoxins. Furthermore, the position of Thr^{87} in HP-AhpC (Thr^{90} of hPrxI) is located approximately at the interface between dimer and dimer, which may be crucial for the formation of HMW complexes. Taken together, these results suggested that HP-AhpC is more similar to mammalian peroxiredoxins than bacterial peroxiredoxins. Conceivably, their functional or enzymatic characteristics may also be closer to eukaryotic peroxiredoxins.

Molecular size estimation of LMW and HMW HP-AhpC

After harvesting and purifying by native Ni–NTA affinity chromatography, the purified rAhpC was analysed by SDS–PAGE, resulting in the estimation of subunit molecular mass of ~26 kDa. However on non-reducing SDS–PAGE, two major bands at ~26 and 45 kDa were detected (data not shown), indicating that the recombinant protein contains one or more intersubunit disulfide bonds, as previously demonstrated (*6*,*23*). By analytical ultracentrifugation (AUC), we further obtained more accurate molecular-size estimation for the rAhpC in 10 mM Tris buffer (pH 7.5). HP-AhpC exhibited only one peak on AUC analysis, showing a sedimentation coefficient of 3.3 S with a calculated molecular mass of ~44 kDa (Fig. 2A). Therefore, the native AhpC under low-salt environments should exist as a dimeric structure.

In our previous study we showed the switch of AhpC to a HMW polymeric form under long-term oxidative stress in the presence of Trx (*9*), here we further measured the approximate size for the HMW forms of AhpC by using gel-filtration HPLC. First, we separated normal AhpC and 10 mM H_2O_2-treated AhpC samples in the presence of Trx–TrxR system by G4000SWXL gel-filtration HPLC, respectively. The results were shown in Fig. 2B. Originally, the native AhpC mixtures were separated into two major peaks: one peak corresponding to a broad spread-out fraction with molecular masses ranged from 45 to 120 kDa and the other one corresponding to 25 kDa. However, when we eluted HP-AhpC pretreated with 10 mM H_2O_2 in the presence of Trx–TrxR system, the original LMW protein peaks disappeared, concomitantly with the appearance of a broad peak of HMW proteins ranging from 700 to over 2,000 kDa. This result was in accord with previous size estimations based on native-PAGE and electron microscopic (EM) analysis (*9*).

Trx-dependent peroxidation-mediated changes in hydrophobicity and secondary structure of HP-AhpC

To protect target substrates from stress-induced aggregation, chaperones bind to unfolding states of substrate proteins. We have shown previously that HP-AhpC can polymerize to form a molecular chaperone under oxidative stress (*9*). Therefore, to address the structural switch of AhpC at molecular level in more details, we used far UV-CD to analyse its secondary structure and *bis*-ANS-mediated fluorescence to measure its degree of exposed hydrophobic-surface under oxidative stress. Under normal condition, the CD spectra of native AhpC exhibited its major secondary structure consisting of α-helix and β-sheet. Nevertheless, after treatment with 10 mM H_2O_2 in the presence of Trx for 1 h, all α-helical domains were greatly reduced while β-sheet domains appeared to be maintained (Fig. 2C).

Regarding *bis*-ANS binding to normal AhpC, we observed that its emission maximum shifted from 520 nm to the shorter wavelength of ~490 nm (Fig. 2D). Subsequently, the fluorescence intensity of *bis*-ANS binding-AhpC was found to significantly increase under oxidative stress, indicating that after peroxidation more hydrophobic patches of AhpC were exposed outside. Therefore, the results point to the fact that AhpC molecules undergo a polymerization process to form HMW chaperone under oxidative stress, accompanied by the unfolding of α-helical

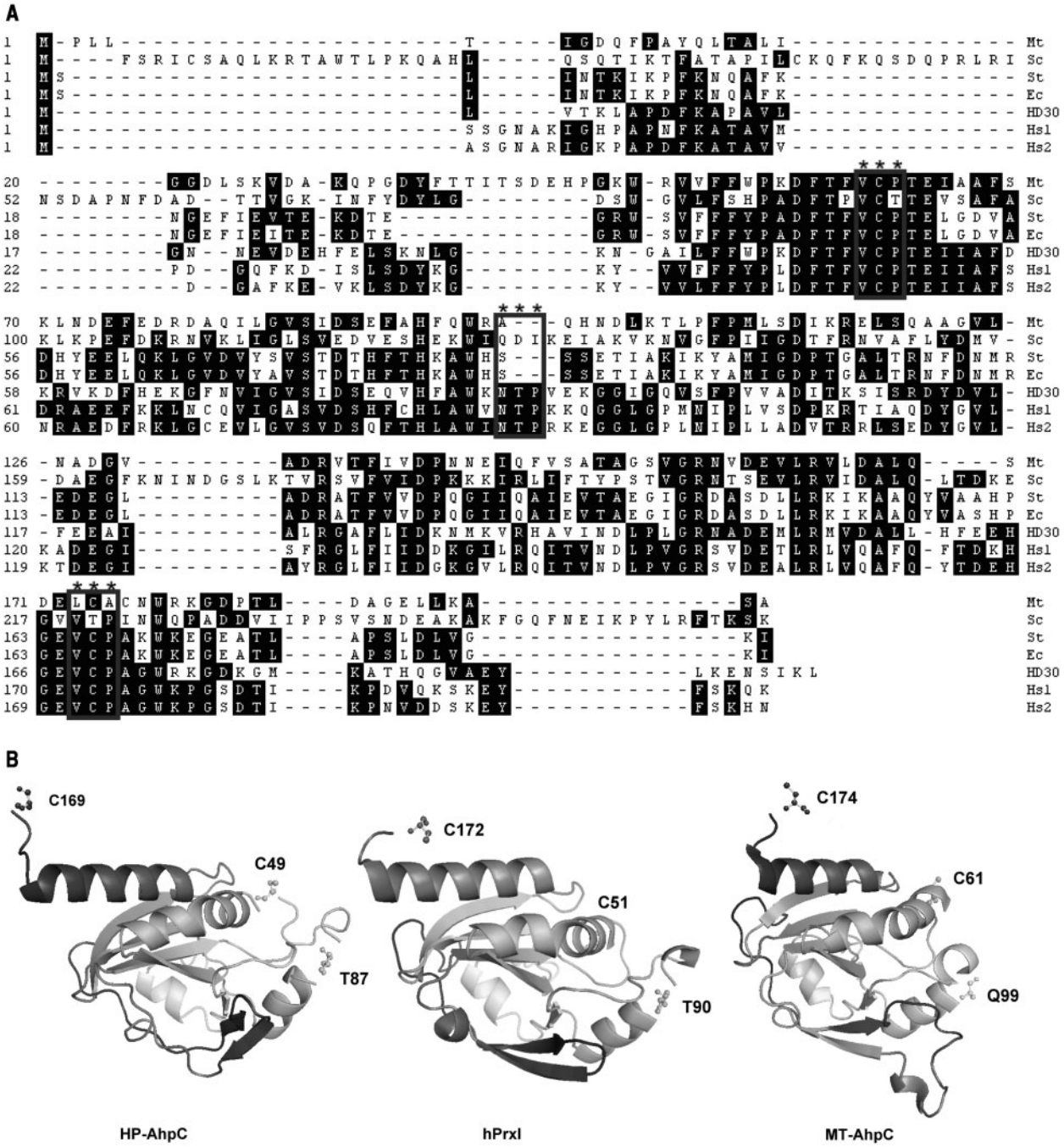

Fig. 1 Sequence alignment and structural comparison of *H. pylori* AhpC with homologous AhpC and Prxs from other species. (A) Alignment of the amino acid sequences of AhpC and Prxs (2-Cys Prx) from several representative prokaryotes and eukaryotes. The encoded amino acid sequences were aligned, and gaps (dashes) were introduced to optimize sequence alignment. Identical and similar amino acids in all sequences are shown in black boxes. The abbreviations for amino acid sequences of AhpC and Prx from various species are as follows: HD30, AhpC of a clinical strain of *H. pylori* studied in this report; Ec, AhpC of *E. coli*; Mt, AhpC of *M. tuberculosis*; St, AhpC of *S. typhimurium*; Sc, Prx I of yeast (*S. cerevisiae*); Hs1, Prx I of human; Hs2, Prx II of human. The regions related to peroxidase and chaperone activities of human peroxiredoxins were designated by three stars (above the enclosed squares). (B) Structures of monomer HP-AhpC (*H. pylori* AhpC), hPrx (human PrxI), and MT-AhpC (*M. tuberculosis* AhpC) are shown as ribbon diagrams. The three residues (C^{49}, C^{169}, T^{87} of HP-AhpC; C^{51}, C^{172}, T^{90} of hPrxI; C^{61}, C^{174}, Q^{99} of MT-AhpC) related to peroxidase and chaperone activities of human peroxiredoxins are displayed as ball-and-stick representation.

domains and disruption of some hydrophilic loops on the surface and exposure of the hydrophobic regions.

Comparative analysis of peroxide reductase activity and changes in molecular size of HP-AhpC and hPrxI

To investigate the functionality of HP-AhpC and hPrxI, wild-type HP-AhpC, mutant HP-AhpC and hPrxI were analysed with respect to their peroxide reductase activities (Fig. 3A). In contrast to HP-AhpC, hPrxI lost its enzyme activity when assayed in the presence of 1 mM H_2O_2. However, HP-AhpC still possessed its peroxide reductase activity even with H_2O_2 concentration higher than 1 mM. Among mutants of HP-AhpC, only C49S enzyme was found

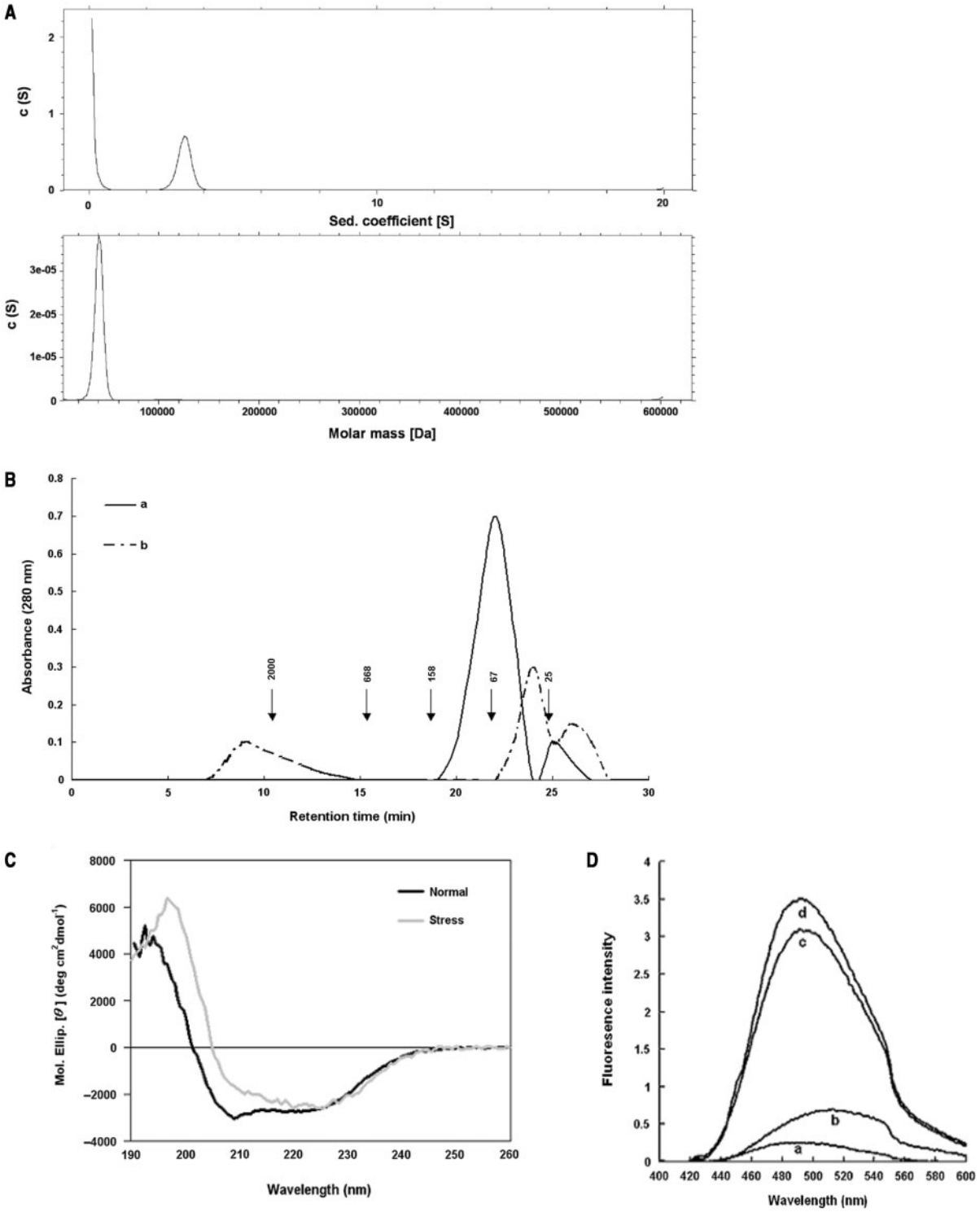

Fig. 2 Changes in molecular size, secondary structure and surface hydrophobicity of HP-AhpC by peroxidation in the presence of Trx. (A) Molecular size of HP-AhpC as analysed by analytical ultracentrifuge (AUC). AUC was performed by a Beckman–Coulter XL-A analytical ultracentrifuge with an An60Ti rotor as described in the 'Materials and Methods' section. The sedimentation coefficient (S) of the native rAhpC was 3.6 S (upper) and its size was calculated to be 44 kDa (lower). All the data were analysed with the SedFit program. (B) Normal native HP-AhpC (line a) and AhpC treated with 10 mM H_2O_2 in the presence of Trx–TrxR system (line b) were analysed using a TSK G4000SWXL HPLC column. The native form of HP-AhpC showed a major peak corresponding to the dimer form and a minor peak corresponding to the monomer. However, HP-AhpC pretreated with 10 mM H_2O_2 in the presence of Trx–TrxR system (*5*) showed a major broad HMW peak ranging from 700 to over 2,000 kDa as estimated by standard MW kit (Blue dextran, 2,000 kDa; Thyroglobulin, 668 kDa; Aldolase, 158 kDa; Albumin, 67 kDa; Chymotrypsinogen A, 25 kDa). It is noted that monomer and dimer peaks did not appear under oxidative stress in line b, indicating the complete conversion of native HP-AhpC to HMW complexes. The other two peaks smaller than 67 kDa in line b were TrxR and Trx, respectively. (C) The far UV-CD spectra of normal (black line) and oxidized (gray line) HP-AhpC. [θ] is the mean molar ellipticity. Note that all the oxidized HP-AhpC (treated with 10 mM H_2O_2) shows a decrease in [θ] at 207 nm, indicating a loss of α-helical structure. (D) The *bis*-ANS-binding fluorescence spectra. Ten micromolar normal HP-AhpC (line a); 5 μM *bis*-ANS (line b); 5 mM *bis*-ANS plus 10 μM normal HP-AhpC (line c); and 5 mM *bis*-ANS plus HP-AhpC pretreated with 10 mM H_2O_2 in the presence of Trx–TrxR system for 10 min (line d).

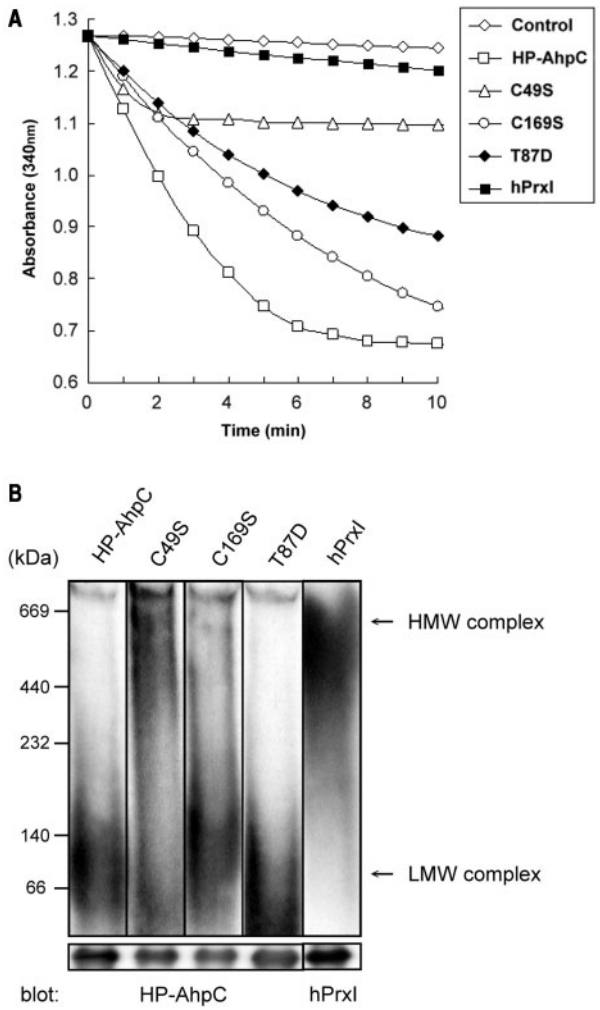

Fig. 3 Comparative analysis of peroxide reductase activity and changes in molecular size of HP-AhpC and hPrxI. (A) Comparison of relative peroxide reductase activity of wild-type HP-AhpC, mutant HP-AhpC (C49S, C169S and T87D) and hPrxI. The peroxide reductase activity of recombinant AhpC was monitored by following the decrease in A_{340} within 10 min due to NADPH oxidation. Each assay was performed by using 20 μM (final concentration) each of AhpC, its mutants or hPrxI in a total volume of 1.0 ml of 50 mM potassium phosphate buffer (pH 7.0)/0.1 M ammonium sulfate/0.5 mM EDTA containing Trx/TrxR system (5 μM thioredoxin, 0.5 μM thioredoxin reductase and 150 μM NADPH) and 1 mM H_2O_2 as described (*9*). The control used here contained only NADPH and H_2O_2. It is noted that the specific activity of HP-AhpC is higher than that of hPrxI and C49S mutant, which shows almost total loss of activity as compared with other mutants. (B) Molecular size of recombinant wild-type HP-AhpC, mutant HP-AhpC (C49S, C169S and T87D) and hPrxI after treatment with 1 mM H_2O_2 in the presence of Trx/TrxR system for 16 h. The 0.2 μg each of oxidized HP-AhpC or hPrxI proteins were analysed by native-PAGE (4–12% gradient polyacrylamide gel) and detected by western blot using antibodies against HP-AhpC (*9*) and human hPrxI (upper panel). Note that only C49S HP-AhpC and hPrxI shows HMW complexes at the upper part of the native gel, indicating the formation of HMW molecular chaperones for these two enzymes (*9*,*10*). All of the different mutants of HP-AhpC and hPrxI showed a 26 kDa single band on 12% SDS–PAGE after western blot (lower panel).

to be inactivated by 1 mM H_2O_2 in 2 min, indicating that the Cys^{169} residue of C49S-HP-AhpC becomes very sensitive to oxidative stress. In other words, the Cys^{49}, not Cys^{169} residue is crucial for the peroxide reductase activity of HP-AhpC to decompose H_2O_2. Unlike hPrxI, we also found that T87D-HP-AhpC did not exhibit a markedly reduced enzyme activity (*14*).

By performing native PAGE followed by western blot, we further examined changes in molecular size of these enzymes. As shown in Fig. 3B, all hPrxI was converted to HMW complexes when exposed to 1 mM H_2O_2. On the other hand, only C49S mutant HP-AhpC showed a significant change in molecular size under oxidative stress, corroborating the result of the reduced peroxide reductase activity for this mutant enzyme under oxidative stress and the higher stability of HP-AhpC towards H_2O_2 than that of hPrxI.

Characterization of oxidized HP-AhpC by 2-DE and LC-MS/MS in vivo

To further characterize whether the mechanism involved in the inactivation of HP-AhpC was similar to that of human peroxiredoxins involving the oxidation of the catalytic-site cysteine to cysteine-sulfinic acid (*12*). We have thus examined the effect of oxidative stress on AhpC in *H. pylori* under *in vivo* conditions and characterized the reaction intermediate(s) by performing 2-DE and LC-MS/MS. As shown in Fig. 4A, the expression level of HP-AhpC increased and the isoelectric point *p*I of HP-AhpC was found to shift to lower pH after treatment with 10 mM H_2O_2 for 3 h. In-gel digestion followed by bioinformatics sequence search/identification of a series of HP-AhpC spots, we found two spots corresponding to peroxidation-modified products Cys^{49}-SO_2H (Fig. 4B) and Cys^{49}-SO_3H (Fig. 4C) at cysteine residues of AhpC, respectively. Therefore, the results corroborated that inactivation of HP-AhpC activity in *H. pylori* under oxidative stress is similar to that of human peroxiredoxins.

Discussion

AhpC is an important antioxidant enzyme of *H. pylori*. Previous literature abounded with reports concerning structure–function correlation of this antioxidant protein with peroxide-reductase activity and its biological roles with other antioxidant enzymes or virulent factors such as catalase and neutrophil-activating protein (NapA) and vice versa (*24*). We have recently reported that AhpC characterized from *H. pylori* possesses dual functionality under normal and oxidative stress conditions (*9*). In this report we would like to address the salient dual-functionality associated with this prokaryote antioxidant enzyme and compare the proposed mechanistic scheme (Fig. 5) underlying its functional switch with that of the well-studied human 2-Cys peroxiredoxins (*11–14*). We have first confirmed that similar to peroxiredoxins, formation of HMW complexes from AhpC polymerization under oxidative stress is Trx-dependent. Treatment of the enzymes under oxidative stress in the presence of Trx can trigger the transition of LMW oligomers of HP-AhpC to HMW complexes ranging from 700 to over 2,000 kDa (Fig. 2B).

We further analysed the secondary-structure and surface-hydrophobicity of AhpC by means of far-UV

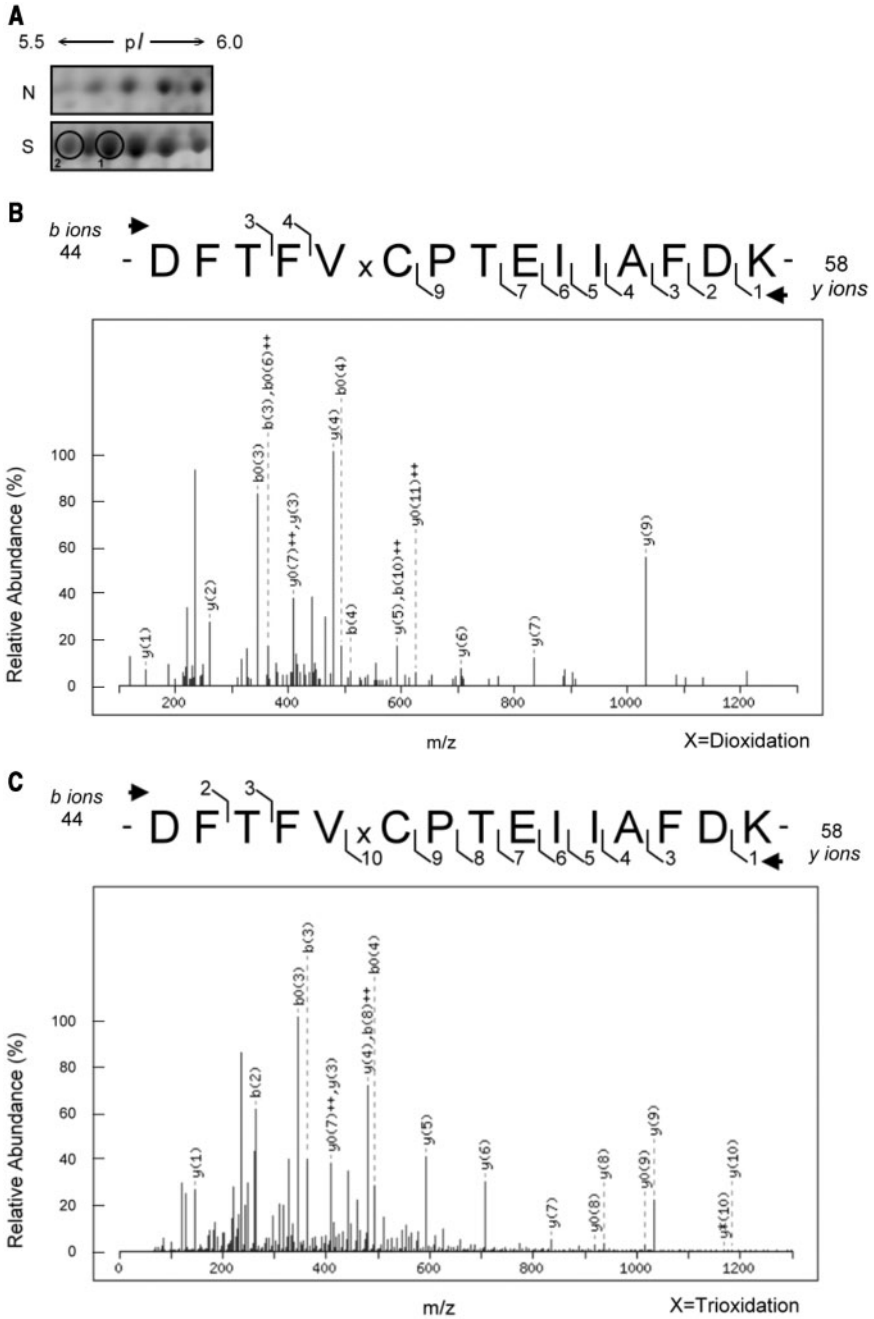

Fig. 4 Identification of *in vivo* oxidized products of HP-AhpC by 2-DE and LC-MS/MS. (A) Two-hundred and fifty microgram total proteins from lysates of *H. pylori* cells were loaded on IPG gel strips (pH 3–10, 13 cm). The sample-loaded IPG strips were rehydrated, subjected to IEF and followed by 2-DE. Only the regions of the Sypro-Ruby stained gels containing HP-AhpC spots are shown. N, normal condition; S, stressed condition (treated with 10 mM H_2O_2 for 3 h). (B) The spectra of the digested peptides from oxidized HP-AhpC (circled No. 1 in panel A) as analysed and plotted by MASCOT database search program. The MS/MS fragmentation pattern shows the presence of the Cys^{49}-containing peptide DFTFVCPTEIIAFDK (mass: 1776.7845 a.m.u.), in which Cys^{49}-SH at the catalytic site has been converted to Cys^{49}-SO_2H. (**C**) The spectra of the digested peptides from oxidized HP-AhpC (circled No. 2 in panel A) as analysed and plotted by MASCOT program. The MS/MS fragmentation pattern shows the presence of the Cys^{49}-containing peptide DFTFVCPTEIIAFDK (mass: 1792.7616 a.m.u.), in which Cys^{49}-SH at the catalytic site has been converted to Cys^{49}-SO_3H.

CD and extrinsic fluorescent probe, i.e. *bis*-ANS dye molecules. As shown in Fig. 2C, α-helical domains in AhpC disappear progressively during the process of Trx-mediated polymerization upon exposure to oxidative stress. Concomitantly, *bis*-ANS mediated protein fluorescence was also found to increase after peroxide treatment in the presence of Trx (Fig. 2D).

Comparative analysis of peroxide reductase activity associated with HP-AhpC and hPrxI showed that HP-AhpC could tolerate a much higher concentration of H_2O_2 (>1 mM H_2O_2) than hPrxI (<1 mM H_2O_2) (Fig. 3A). In our unpublished data, we also found that *H. pylori* could resist the oxidative treatment up to 10 mM H_2O_2 whereas human gastric epithelial cell

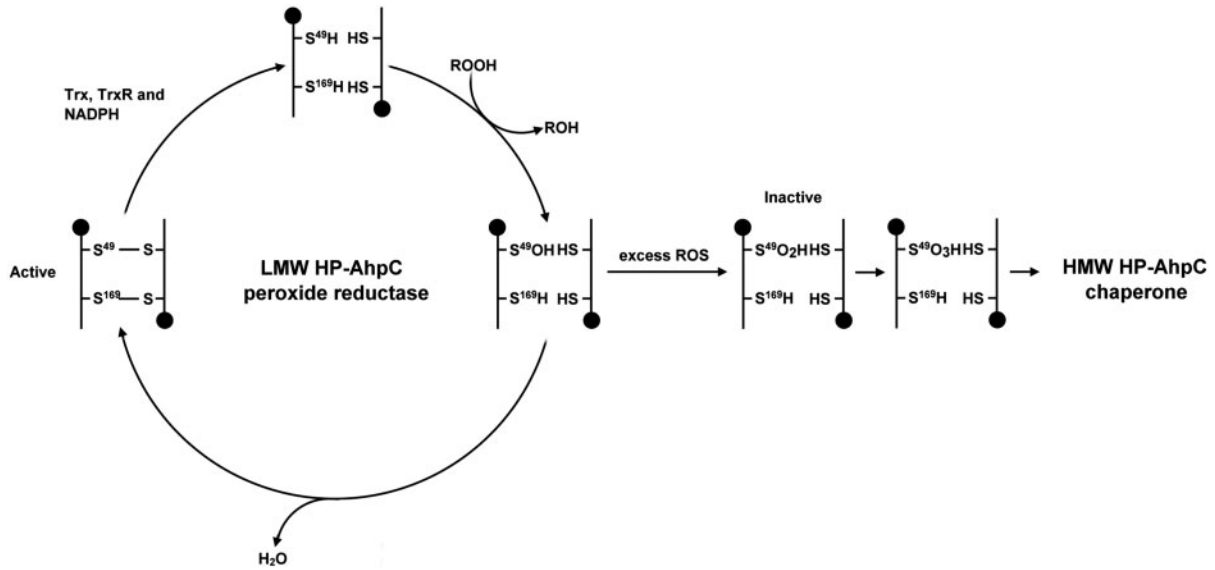

Fig. 5 A schematic representation of the peroxidation-induced functional switch for AhpC with dual functionality in *H. pylori*. Under normal cellular environment, LMW HP-AhpC efficiently reduces toxic ROS by its peroxide reductase or peroxidase activity through a canonical reaction cycle by coupling reactions involving Trx, TrxR and NADPH. When cells encounter oxidative stress, LMW HP-AhpC initially undergoes a peroxidative reaction cycle and becomes peroxidized, converting cysteine at its active site to cysteine sulfinic acid (-SO_2H) and sulfonic acid (-SO_3H). The oxidized LMW HP-AhpC would become denatured and unfolded, accompanied by its being converted to HMW complexes with chaperone activity for prevention of mis- or un-folded proteins from aggregation.

(AGS cells) could only survive at H_2O_2 concentration <1 mM. Therefore the prokaryote AhpC is more stable to oxidative stress than human peroxiredoxins regarding its peroxide-decomposing capability and cell-protection potential.

Polymerization of hPrxI to HMW chaperone was found to be accompanied by enzyme inactivation and phosphorylation of Thr^{90} (*10*, *12–14*). In contrast to wild-type HP-AhpC and site-specific mutant at Cys^{169} (C169S-HP-AhpC), C49S-HP-AhpC mutant was found to form HMW complexes easily inactivated by 1 mM H_2O_2 (Fig. 3), indicating that the crucial active site for AhpC activity is located at Cys^{49}. Meanwhile, C49S mutant of HP-AhpC is also prone to undergoing polymerization to form HMW complexes. Characterization of oxidized HP-AhpC *in vivo* after treatment of *H. pylori* with H_2O_2 revealed that Cys^{49} was converted to Cys^{49}-SO_2H and Cys^{49}-SO_3H under oxidative stress (Fig. 4). Similarly, irreversible oxidation of the active-site cysteine of peroxiredoxin to cysteine sulfonic acid abolishes the enzyme activity, accompanied by an increase in chaperone activity as demonstrated previously (*13*). The peroxidation of the catalytic-site Cys^{51}-SH to Cys^{51}-SO_2H in hPrxI was found to be reversed by sulfiredoxin (*25*, *26*), resulting in the recovery of thiol group. We did not find any homologous gene like human sulfiredoxin after a comprehensive search in *H. pylori* genome by using bioinformatics BLAST program. Therefore, whether there exists a mechanism for the reversible or irreversible oxidation of active site in HP-AhpC remained to be answered in the future.

Lastly, we also address the role of phosphorylation in relation to the formation of HMW chaperone by site-specific mutation of Thr^{87} to Asp^{87} mimicking the phosphorylation status of the enzyme. In contrast to human peroxiredoxins, we did not find any significant difference between this mutant enzyme and wild-type HP-AhpC in spite of high sequence similarity in the region enclosing Thr^{87} in HP-AhpC and Thr^{90} in hPrxI. In conclusion, a detailed study of the functional variation and evolution of HP-AhpC as compared with that of homologous human peroxiredoxins may provide some insights into the mechanism underlying the development of dual functionalities for this family of 2-Cys peroxiredoxin.

Acknowledgements

The authors thank Dr Ming-Shiang Wu and Dr Jaw-Town Lin of the Division of Gastroenterology, National Taiwan University Hospital for providing the clinical isolates of *H. pylori* in this study.

Funding

Academia and the National Science Council (NSC Grant 96-2311-B-037-005-MY3 to S.-H. Chiou), Taipei, Taiwan.

Conflict of interest

None declared.

References

1. Wood, Z.A., Schroder, E., Robin Harris, J., and Poole, L.B. (2003) Structure, mechanism and regulation of peroxiredoxins. *Trends Biochem. Sci.* **28**, 32–40
2. Olczak, A.A., Seyler, R.W. Jr., Olson, J.W., and Maier, R.J. (2003) Association of *Helicobacter pylori* antioxidant activities with host colonization proficiency. *Infect. Immun.* **71**, 580–583
3. Suzuki, H., and Hibi, T. (2006) Oxidative stress in *Helicobacter pylori*-associated gastroduodenal disease. *J. Clin. Biochem. Nutr.* **39**, 56–63
4. Handa, O., Naito, Y., and Yoshikawa, T. (2007) CagA protein of *Helicobacter pylori*: a hijacker of gastric

epithelial cell signaling. *Biochem. Pharmacol.* **73**, 1697–1702
5. Baker, L.M., Raudonikiene, A., Hoffman, P.S., and Poole, L.B. (2001) Essential thioredoxin-dependent peroxiredoxin system from *Helicobacter pylori*: genetic and kinetic characterization. *J. Bacteriol.* **183**, 1961–1973
6. Wang, G., Olczak, A.A., Walton, J.P., and Maier, R.J. (2005) Contribution of the *Helicobacter pylori* thiol peroxidase bacterioferritin comigratory protein to oxidative stress resistance and host colonization. *Infect. Immun.* **73**, 378–384
7. Reynolds, C.M., and Poole, L.B. (2001) Activity of one of two engineered heterodimers of AhpF, the NADH:peroxiredoxin oxidoreductase from Salmonella typhimurium, reveals intrasubunit electron transfer between domains. *Biochemistry* **40**, 3912–3919
8. Koshkin, A., Knudsen, G.M., and Ortiz De Montellano, P.R. (2004) Intermolecular interactions in the AhpC/AhpD antioxidant defense system of Mycobacterium tuberculosis. *Arch. Biochem. Biophys.* **427**, 41–47
9. Chuang, M.H., Wu, M.S., Lo, W.L., Lin, J.T., Wong, C.H., and Chiou, S.H. (2006) The antioxidant protein alkylhydroperoxide reductase of *Helicobacter pylori* switches from a peroxide reductase to a molecular chaperone function. *Proc. Natl Acad. Sci. USA* **103**, 2552–2557
10. Jang, H.H., Lee, K.O., Chi, Y.H., Jung, B.G., Park, S.K., Park, J.H., Lee, J.R., Lee, S.S., Moon, J.C., Yun, J.W., Choi, Y.O., Kim, W.Y., Kang, J.S., Cheong, G.W., Yun, D.J., Rhee, S.G., Cho, M.J., and Lee, S.Y. (2004) Two enzymes in one; two yeast peroxiredoxins display oxidative stress-dependent switching from a peroxidase to a molecular chaperone function. *Cell* **117**, 625–635
11. Moon, J.C., Hah, Y.S., Kim, W.Y., Jung, B.G., Jang, H.H., Lee, J.R., Kim, S.Y., Lee, Y.M., Jeon, M.G., Kim, C.W., Cho, M.J., and Lee, S.Y. (2005) Oxidative stress-dependent structural and functional switching of a human 2-Cys peroxiredoxin isotype II that enhances HeLa cell resistance to H2O2-induced cell death. *J. Biol. Chem.* **280**, 28775–28784
12. Yang, K.S., Kang, S.W., Woo, H.A., Hwang, S.C., Chae, H.Z., Kim, K., and Rhee, S.G. (2002) Inactivation of human peroxiredoxin I during catalysis as the result of the oxidation of the catalytic site cysteine to cysteine-sulfinic acid. *J. Biol. Chem.* **277**, 38029–38036
13. Lim, J.C., Choi, H.I., Park, Y.S., Nam, H.W., Woo, H.A., Kwon, K.S., Kim, Y.S., Rhee, S.G., Kim, K., and Chae, H.Z. (2008) Irreversible oxidation of the active-site cysteine of peroxiredoxin to cysteine sulfonic acid for enhanced molecular chaperone activity. *J. Biol. Chem.* **283**, 28873–28880
14. Jang, H.H., Kim, S.Y., Park, S.K., Jeon, H.S., Lee, Y.M., Jung, J.H., Lee, S.Y., Chae, H.B., Jung, Y.J., Lee, K.O., Lim, C.O., Chung, W.S., Bahk, J.D., Yun, D.J., Cho, M.J., and Lee, S.Y. (2006) Phosphorylation and concomitant structural changes in human 2-Cys peroxiredoxin isotype I differentially regulate its peroxidase and molecular chaperone functions. *FEBS Lett.* **580**, 351–355
15. Kang, S.W., Rhee, S.G., Chang, T.S., Jeong, W., and Choi, M.H. (2005) 2-Cys peroxiredoxin function in intracellular signal transduction: therapeutic implications. *Trends Mol. Med.* **11**, 571–578
16. Schwede, T., Kopp, J., Guex, N., and Peitsch, M.C. (2003) SWISS-MODEL: An automated protein homology-modeling server. *Nucleic Acids Res.* **31**, 3381–3385
17. Altschul, S.F., Madden, T.L., Schaffer, A.A., Zhang, J., Zhang, Z., Miller, W., and Lipman, D.J. (1997) Gapped BLAST and PSI-BLAST: a new generation of protein database search programs. *Nucleic Acids Res.* **25**, 3389–3402
18. Papinutto, E., Windle, H.J., Cendron, L., Battistutta, R., Kelleher, D., and Zanotti, G. (2005) Crystal structure of alkyl hydroperoxide-reductase (AhpC) from *Helicobacter pylori*. *Biochim. Biophys. Acta* **1753**, 240–246
19. Schroder, E., Littlechild, J.A., Lebedev, A.A., Errington, N., Vagin, A.A., and Isupov, M.N. (2000) Crystal structure of decameric 2-Cys peroxiredoxin from human erythrocytes at 1.7 A resolution. *Structure* **8**, 605–615
20. Guimaraes, B.G., Souchon, H., Honore, N., Saint-Joanis, B., Brosch, R., Shepard, W., Cole, S.T., and Alzari, P.M. (2005) Structure and mechanism of the alkyl hydroperoxidase AhpC, a key element of the Mycobacterium tuberculosis defense system against oxidative stress. *J. Biol. Chem.* **280**, 25735–25742
21. Yu, C.M., Chang, G.G., Chang, H.C., and Chiou, S.H. (2004) Cloning and characterization of a thermostable catfish alphaB-crystallin with chaperone-like activity at high temperatures. *Exp. Eye Res.* **79**, 249–261
22. Chuang, M.H., Chiou, S.H., Huang, C.H., Yang, W.B., and Wong, C.H. (2009) The lifespan-promoting effect of acetic acid and Reishi polysaccharide. *Bioorg. Med. Chem.* **17**, 7831–7840
23. Olczak, A.A., Olson, J.W., and Maier, R.J. (2002) Oxidative-stress resistance mutants of *Helicobacter pylori*. *J. Bacteriol.* **184**, 3186–3193
24. Wang, G., Alamuri, P., and Maier, R.J. (2006) The diverse antioxidant systems of *Helicobacter pylori*. *Mol. Microbiol.* **61**, 847–860
25. Chang, T.S., Jeong, W., Woo, H.A., Lee, S.M., Park, S., and Rhee, S.G. (2004) Characterization of mammalian sulfiredoxin and its reactivation of hyperoxidized peroxiredoxin through reduction of cysteine sulfinic acid in the active site to cysteine. *J. Biol. Chem.* **279**, 50994–51001
26. Biteau, B., Labarre, J., and Toledano, M.B. (2003) ATP-dependent reduction of cysteine-sulphinic acid by S. cerevisiae sulphiredoxin. *Nature* **425**, 980–984